

Accepted Manuscript

Tungstate-loaded triazine-based magnetic Poly(Bis-imidazolium ionic liquid):
An effective Bi-Functional catalyst for tandem selective oxidation/Knoevenagel
condensation in water

Nasrin Zohreh, Maryam Tavakolizadeh, Seyed Hassan Hosseini, Ali Pourjavadi, Craig
Bennett

PII: S0032-3861(17)30151-9

DOI: [10.1016/j.polymer.2017.02.028](https://doi.org/10.1016/j.polymer.2017.02.028)

Reference: JPOL 19429

To appear in: *Polymer*

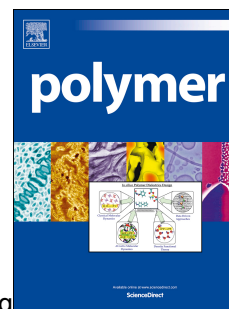
Received Date: 15 December 2016

Revised Date: 3 February 2017

Accepted Date: 7 February 2017

Please cite this article as: Zohreh N, Tavakolizadeh M, Hosseini SH, Pourjavadi A, Bennett C, Tungstate-loaded triazine-based magnetic Poly(Bis-imidazolium ionic liquid): An effective Bi-Functional catalyst for tandem selective oxidation/Knoevenagel condensation in water, *Polymer* (2017), doi: [10.1016/j.polymer.2017.02.028](https://doi.org/10.1016/j.polymer.2017.02.028).

This is a PDF file of an unedited manuscript that has been accepted for publication. As a service to our customers we are providing this early version of the manuscript. The manuscript will undergo copyediting, typesetting, and review of the resulting proof before it is published in its final form. Please note that during the production process errors may be discovered which could affect the content, and all legal disclaimers that apply to the journal pertain.



Tungstate-Loaded Triazine-Based Magnetic Poly(Bis-imidazolium Ionic Liquid): An Effective Bi-Functional Catalyst for Tandem Selective Oxidation/Knoevenagel Condensation in Water

Nasrin Zohreh,^{*,[a]} Maryam Tavakolizadeh,^[a] Seyed Hassan Hosseini,^[b] Ali Pourjavadi,^[b] Craig Bennett^[c]

^[a] *Department of Chemistry, Faculty of Science, University of Qom, P. O. Box: 37185-359, Qom, Iran*

^[b] *Polymer Research Laboratory, Department of Chemistry, Sharif University of Technology, Tehran, Iran*

^[c] *Department of Physics, Acadia University, Wolfville, Nova Scotia, Canada*

(E-mail address: nasrin.zohreh@gmail.com, n.zohreh@qom.ac.ir; Phone/fax: +982532103488)

Abstract

A novel bi-functional polymeric catalyst was synthesized by immobilization of tungstate anions onto the nitrogen rich poly(ionic liquid)/magnetic nanocomposite. The resulting catalyst has two types of catalytic sites: (i) immobilized WO₄ anions with bis-imidazolium ionic liquid cation for selective oxidation of alcohols and (ii) basic amine groups for Knoevenagel condensation between produced aldehyde and malononitrile. Due to the polymeric nature of the catalyst, large amounts of tungstate and basic nitrogen groups were presented on the solid surface which led to a decrease in the applied catalyst mass for catalytic reaction. High catalytic activity and excellent selectivity of catalyst in water medium make this protocol a green way for production of fine chemicals.

Keywords: Bi-functional catalyst; Magnetic catalyst; Oxidation; Knoevenagel condensation

1. Introduction

The remarkable physicochemical properties of ionic liquids (ILs) make them unique materials for various applications.[1-9] Over the last decade, many efforts have been made to develop the application of ILs in the area of catalysis.[5, 6, 10-13] However, these specific homogenous IL catalysts are minimally recyclable and, therefore, are not desirable for industrial applications.[14-16] A standard solution for the recyclability issue is immobilization of homogenous IL catalysts onto solid insoluble supports such as silica particles,[17-20] carbon-based materials[21-23] and magnetic nanoparticles (MNPs).[24-26] The last approach is most desirable because their magnetic property facilitates the catalyst separation using an external magnet.[25, 27-31] Despite excellent recyclability and good catalytic performance of these supported IL catalysts, there is one unsolved issue which has limited their widespread application. Since the surface areas of solid supports are defined, they can only bear a limited quantity of IL molecules and therefore the loading amounts of active catalytic species is usually very low in these catalysts.[25, 32, 33] As a result, for a specific catalytic reaction, a large mass of such supported catalyst is needed which leads to use of more solvent for mixing and product separation. To solve the low loading problem, we have recently developed coating of MNPs by poly(ionic liquids) (PILs).[34-39] Coating of solid supports with polymers increases the loading of active catalytic sites (which usually are monomers of polymers).[40] The polymer chains can be covalently bonded to the surface of the solid support by the head while the tail of the polymer chain can be grown without considering the limited surface area.

One of the important organic transformations in industries and laboratories is selective oxidation of substrates such as alcohols to the corresponding aldehydes.[41-46] The classical oxidation methods include the use of stoichiometric amounts of strong oxidants such as chromium (VI)

reagents [47, 48] and concentrated HNO_3 [49] which are environmentally hazardous and produce large amounts of toxic wastes. A green protocol to replace the classical method for oxidation reaction is using heterogeneous oxidation metal catalysts.[50-53] Some of these protocols are based on the use of H_2O_2 as co-catalyst which produces water as the only byproduct.[54-56] However, for selective oxidations, H_2O_2 should be applied in combination with metal catalysts.[57-63] The most effective catalyst for oxidation reactions along with H_2O_2 is tungstate anions.[38, 64-70] However, the difference in solubility of tungstate anion and organic substrates necessitates the use of phase transfer catalysts for these types of catalytic oxidations.[71, 72] However, the recyclability of homogenous catalysts and phase transfer catalysts is still a major problem.[54, 65, 72] A logical approach to this problem is heterogenization of the phase transfer catalyst and tungstate anions.

In this work we have prepared a heterogeneous magnetic catalyst in which bis-imidazolium tungstate ligands were immobilized onto the polymer coated MNPs. Using polymer coated MNP as the support increased the loading amounts of immobilized tungstate anions. This catalyst was then applied for one-pot tandem oxidation/Knoevenagel condensation between various alcohols and active methylene compounds using H_2O_2 as co-oxidant in water medium.[73-77] The mechanism for the tandem reaction was also proposed. This study highlights the great potential of polymer coated magnetic nanoparticles as bi-functional catalysts.

2. Experimental

2.1. Reagents and analysis

Azobisisobutyronitrile (AIBN, Kanto, 97%) was recrystallized from ethanol. Methyl acrylate (MA) and *N*-methylimidazole (NMI) were distilled before use (Sigma-Aldrich). *N,N'*-

methylenebisacrylamide (MBA), trichlorotriazine (TCT) and all other chemical compounds were obtained from Merck and used without further purification.

The chemical structures of the samples were characterized by Fourier transform infrared (FT-IR) spectroscopy using an ABB Bomem MB-100 spectrometer. Thermal gravimetric analysis (TGA) was performed using a TGA Q 50 thermogravimetric analyzer with a heating rate of $10\text{ }^{\circ}\text{C min}^{-1}$ under a nitrogen atmosphere. A Philips CM30 transmission electron microscope (TEM) was used to investigate the morphology of nanoparticles. Magnetization of the samples was measured by vibrating sample magnetometer (Meghnatis Daghigh Kavir Co., Kashan, Iran). Tungstate ions were measured by inductively coupled plasma-optical emission spectrometry (ICP-OES, Perkin-Elmer DV 4300). The X-ray diffraction (XRD) patterns were recorded on a RigakuD/Max-3c X-ray diffractometer. An X-ray fluorescence (XRF) (Philips 1404) was used for accurate elemental analysis of samples. The products were determined by GC (Agilent) equipped with a flame ionization detector using a HP-5 capillary column.

2.2. Synthesis of catalyst (MNP@PIL/W)

Silica coated Fe_3O_4 nanoparticles (MNPs) were synthesized based on our previously reported method.[78] MNP (1.0 g) was ultrasonically dispersed in dry ethanol (50 mL) and then NH_3 (2 mL) was added to flask. Subsequently, 3-(trimethoxysilyl)propylmethacrylate (MPS) (3 mL) was added and the mixture was stirred at $70\text{ }^{\circ}\text{C}$ for 48 h. The MPS coated MNPs (MNP@MPS) were magnetically separated and washed several times with methanol ($4 \times 50\text{ mL}$) and dried under vacuum at $50\text{ }^{\circ}\text{C}$.

Poly(aminoethyl acrylamide) coated MNPs was prepared based on our previous work.[79] In a 500 mL single-necked flask, a solution of MNP@MPS (0.50 g in 200 mL methanol), 2 g methyl

acrylate, 0.5 g of MBA, and 70 mg of AIBN were mixed. The flask was completely deoxygenated by bubbling purified argon for 30 min and then equipped with a fractionating column, Liebig condenser, and a receiver. The polymerization process initiated when heating the flask from ambient temperature to the boiling state in an oil bath. The reaction was ended after about 130 mL of methanol was distilled from the reaction mixture within 5 h. The obtained cross-linked poly(methylacrylate) coated MNP (MNP@PMA) were magnetically separated and washed with water (2×100 mL) and methanol (3×50 mL) and dried under vacuum at 50 °C (1.31 g product).

Subsequently, about 1.0 g of MNP@PMA was ultrasonically dispersed in 60 mL methanol, 25 mL ethylenediamine (EDA) was slowly added and the mixture was stirred at 60 °C for 72 h. Cross-linked poly(aminoethyl acrylamide) coated MNP (denoted as MNP@PAEAm) was magnetically separated and washed with methanol (3×50 mL) and then dried under vacuum at 50 °C for 12 h (0.88 g product).

In a round bottom flask, MNP@PAEAm (0.50 g) was ultrasonically dispersed in dry THF (30 mL). Following this, TCT (2.6 g, 14.0 mmol) and *N,N'*-diisopropylethylenediamine (2.6 mL, 20.0 mmol) were added and the flask was put in an ice bath. The mixture was stirred for 7 h under N₂ atmosphere. The product (MNP@PTCT) was magnetically separated and washed with THF (5×15 mL) and dried under vacuum at room temperature (0.49 g).

Afterward, in a three-necked round bottom flask, MNP@PTCT (0.40 g) was dispersed in dry CH₃CN (25 mL) and NMI (2 mL, 24 mmol) was added to flask. The flask was equipped with a condenser and the mixture was refluxed for 2 days to produce MNP@PIL/Cl. The product was separated using a magnet, washed with methanol (5×10 mL) and dried under vacuum at 50 °C (0.39 g).

For exchange of chloride with tungstate, MNP@PIL/Cl (0.30 g) was dispersed in DI water (25 mL) and $\text{Na}_2\text{WO}_4 \cdot 4\text{H}_2\text{O}$ (0.30 g, 0.82 mmol) was added to mixture. The mixture was stirred for 2 days at room temperature. The final product (MNP@PIL/W) was magnetically separated and washed with water (5×10 mL) and methanol (5×10 mL) and dried under vacuum at 50°C (0.29 g).

2.3. General procedure for one-pot tandem oxidation/ Knoevenagel condensation catalyzed by MNP@PIL/W

In a round-bottomed flask, 0.5 mmol alcohol, 0.75 mmol H_2O_2 , 2 mL solvent water and 4 mol% MNP@PIL/W (26 mg) were mixed and stirred at 90°C for a defined time. After the completion of the reaction, monitored by TLC, the reaction was cooled down to room temperature and then 0.6 mmol malononitrile was added to solution and the mixture was stirred for another 2h. Ethyl acetate was then added to the mixture and catalyst was separated by an external magnet and washed with methanol, dried at 50°C and stored for another run. The product was extracted by ethyl acetate and analyzed by gas chromatography (GC).

3. Results and Discussion

The catalyst was prepared in a few steps (scheme 1). First silica coated magnetic nanoparticles (MNPs) were prepared. Magnetic particles were then functionalized by MPS to generate vinyl groups on the surface of the MNPs. The presence of vinyl groups on the surface of the MNPs allow the covalent grafting of polymer chains to magnetic particles. The cross-linked poly(methyl acrylate) (PMA) coated MNP was prepared through the distillation-precipitation-polymerization method using MA, MBA and AIBN as monomer, cross-linker and initiator in the presence of MNP@MPS as core. The resulting MNP@PMA was reacted with an excess amount

of EDA and cross-linked poly(amino ethyl acrylamide) coated MNP was synthesized (MNP@PAEAm). Coating of MNPs with PAEAm produces a magnetic support with numerous amine groups on the surface. To immobilize tungstate ions, an ionic ligand should be initially attached onto the surface of the support. For this purpose, a bis-imidazolium ligand was grafted to MNP@PAEAm as depicted in scheme 1. After exchange of chloride with tungstate anion, the final catalyst was ready (MNP@PIL/W).

Scheme 1

In each step of synthesis of the catalyst, FT-IR spectroscopy was used to verify the structure of the sample. Figure S1 shows the FT-IR spectra of MNP(a), MNP@MPS (b), MNP@PMA (c) and MNP@PAEAm (d). The characteristic bands within 635, 1106, and 3200-3500 cm^{-1} in all samples are attributed to stretching vibration of Fe-O, Si-O-Si, and O-H, respectively. The FT-IR spectrum of MNP@MPS showed absorption peaks at 1461 and 1713 cm^{-1} attributed to C=C and C=O bonds of MPS and confirmed the grafting of MPS. In the FT-IR spectrum of MNP@PMA, the characteristic peak of cross-linked poly(methyl acrylate) can be seen at 1735 cm^{-1} attributed to ester groups. This also was confirmed by the increasing intensity of the absorption peak at 2929 related to stretching of the C-H bond of alkyl groups. Amidation of CO_2Me functional groups of the polymer shell by ethylenediamine led to a decrease in C=O bond stretching band and appearance of amidic C=O band at 1654 cm^{-1} in the MNP@AEAm spectrum. However, some of the ester groups in the inner layer of the cross-linked polymer shell did not react with EDA. These spectra show the characteristic peaks of each sample confirming the successful synthesis of MNP@PAEAm.

In the next steps, amine groups on the surface of MNP@PAEAm were reacted with TCT and then N-methyl imidazole group added to this structure. The FT-IR spectra of these two steps are shown in Figure 1b and c, but unfortunately the main characteristic peaks of TCT and bis-imidazolium ligand are overlapped by strong peaks of PAEAm. However, after exchange of chloride with tungstate, a peak at 896 cm^{-1} was observed that is attributed to stretching vibration of W=O (comparing with FT-IR of Na_2WO_4 , Figure 1e).

Figure 1

The TG analysis of samples in each step of synthesis of the catalyst shows that, after each modification on the surface of the MNPs, weight loss increases (Figure 2). The TGA analysis of MNP@MPS shows 2.20 % total weight loss at $250\text{ }^\circ\text{C}$ (Figure 2a). From this weight loss, the loading amount of MPS on the surface of MNPs was calculated as 0.17 mmol/g. All samples show a weight loss at $100\text{ }^\circ\text{C}$ which is attributed to loss of adsorbed water molecules. After this, the main weight losses occur at around $300\text{ }^\circ\text{C}$ which is associated with degradation of all organic components on the samples. The TGA curves of MNP@PMA, MNP@PAEAm, MNP@PTCT and MNP@PIL/W show 17.9, 24.0, 38.4 and 43.1% weight losses, respectively (Figure 2b-e). Due to the different structure of monomer and cross-linker on the surface of each sample, the exact calculation of loading amount of each part is not possible. However, the results of TGA clearly show that modification was successfully performed in each step of catalyst preparation.

Figure 2

Table 1 shows the elemental analysis of MNP@MPS, MNP@PMA, MNP@PAEAm, MNP@TCT and MNP@PIL/W. CHN analysis shows that content of C, H and N after each

modification increases confirming the successful modification in each step. The XRF analysis shows 6.43 wt% chloride in the MNP@PTCT sample which is related to two unreacted chlorides of grafted TCT molecules. From the weight percent of chloride, it can be concluded that the loading amount of immobilized TCT on MNP@PTCT is around 0.91 mmol/g. Moreover, it was found that the amounts of W and Cl in MNP@PIL/W are 0.59 and 14.09 wt%. The content of W in this sample is related to 0.77 mmol/g of WO_4 anions. Reduction of the Cl content in this sample shows the successful exchange of WO_4 with chlorides. Moreover, the XRF analysis of MNP@PIL/W did not detect any Na, confirming that there is no NaWO_4^- or un-exchanged Na_2WO_4 . These results show that WO_4^{2-} is paired to one bis-imidazolium ligand.

Assuming that the only nitrogen source in MNP@PMA is MBA cross-linker, the amount of cross-linking in MNP@PMA can be calculated using the N content of sample. It was found that the content of MBA in MNP@PMA is about 1.84 wt%. Along with the TGA data (Figure 2b), the content of poly(methyl acrylate) in MNP@PMA is about 13.86 wt% which is related to 1.61 mmol/g of CO_2Me groups in $(17.9 - 2.2 - 1.84 = 13.86)$. Based on these results, the amount of ethylenediamine in MNP@PAEAm was calculated as 1.24 mmol/g. The content of available amine groups on the surface of MNP@PAEAm was also calculated by the back titration method and it was found to be 1.11 mmol/g which is in a good agreement with the NH_2 content calculated based on CHN analysis (see supporting information). The results of ICP analysis also showed 14.19 wt% of W in MNP@PIL/W which is closely agrees with the results of XRF.

Table 1

EDS analysis of MNP@PIL/W confirms the presence of C, N, O, Fe, Si and W (Figure 3). The absence of Na and Cl in EDS analysis demonstrates that the ratio of bis-imidazolium cation to WO_4 anion is 2:1. Moreover, the absence of Na in this analysis shows that there is no physically

adsorbed Na_2WO_4 on the surface of catalyst. These results are in good agreements with the XRF analysis.

Figure 3

TEM images of Fe_3O_4 nanoparticles and MNP@PIL/W are presented in Figure 4a and b, respectively. As shown, the size of magnetic Fe_3O_4 nanoparticle is less than 10 nm (Figure 4a). The TEM image of MNP@PIL/W shows gray material around the dark Fe_3O_4 nanoparticles. Based on the TEM analysis, the size of catalyst is more than 130 nm and several Fe_3O_4 nanoparticles are entrapped within the polymeric matrix.

Figure 4

The XRD analysis of MNP@PIL/W (Figure 5a) shows that, the locations and intensities of the diffraction peaks are identical to that of the pure Fe_3O_4 nanoparticle sample and consistent with the standard pattern (JCPDS Card No. 79 - 0417 magnetite). The broad peak between 20-30 degrees is attributed to amorphous silica and the polymeric shell. This pattern shows that the crystalline phase of Fe_3O_4 did not change during the catalyst preparation steps. The electron diffraction pattern (RDP) of MNP@PIL/W also confirms the crystalline structure of the Fe_3O_4 nanoparticles (Figure 5b)

Figure 5

Figure 6 shows the hysteresis loops of pure Fe_3O_4 (a) and MNP@PIL/W (b) at room temperature. The maximum saturation magnetization of Fe_3O_4 and MNP@PIL/W are 54.2 and 20.4 emu/g, respectively. The large decrease of saturation magnetization of MNP@PIL/W is attributed to coating of non-magnetic silica and polymer shells around the magnetic

nanoparticles. Even with this reduction in the saturation magnetization, MNP@PIL/W can still be easily separated from the solution by using an external magnet.

Figure 6

One-pot reactions catalyzed by multi-functional heterogeneous catalysts are an important strategy for industrial production since they do not require isolation and purification of intermediates, facilitating a greener process. The catalytic activity of MNP@PIL/W as a bi-functional catalyst was examined in tandem oxidation/Knoevenagel condensation between benzyl alcohol and malononitrile. This reaction can be performed in two steps under one-pot condition: first, oxidation of benzyl alcohol and, second, amine promoted Knoevenagel condensation to yield 2-benzylidenemalononitrile. Table 2 shows a control experiment for a model reaction between benzyl alcohol and malononitrile. The reaction in the absence of catalyst or un-supported Na_2WO_4 gave no significant conversion of benzyl alcohol (Entry 1,2), confirming that the oxidation of alcohol needs a phase transfer catalyst along with tungstate catalyst. Using MNP@PIL/Cl gave only a 13% conversion to a mixture of benzaldehyde and benzoic acid (Entry 3). However, using 5 mol% of MNP@PIL/W converts more than 96% of the benzyl alcohol and produces 96% yield of desired product. The reaction gave almost same the conversion with 4 mol% catalyst but reducing the amount of MNP@PIL/W to 3 mol% reduced the conversion of alcohol to 87%. However, Knoevenagel condensation of produced benzaldehyde was complete at this condition (Entry 6). In the next step, reaction time for each step was optimized and it was found that oxidation reaction (Time A) and Knoevenagel condensation (Time B) needs at least 4h and 2 h for completion, respectively (Entry 5,7-9). The same reaction was performed in various solvents instead of water but the best result was obtained in water (Entry 10-13). To understand the effect of the catalyst in tandem reaction, two other

experiments were performed using benzaldehyde as the starting substrate (Entry 14,15). To understand the effect of MNPs in catalytic activity of MNP@PIL/W, same catalyst was prepared without the MNPs. The result showed that the absence of MNPs in catalyst structure did not significantly affect on yield of products (Entry 16). The first experiment demonstrates that Knoevenagel condensation did not proceed in the absence of any catalyst. In contrast, using MNP@PIL/Cl without tungstate anion gave 99% yield of Knoevenagel product when the reaction started with benzaldehyde instead of benzyl alcohol. This result confirms that tungstate anions are not responsible for Knoevenagel condensation and that the basic amine groups on the surface of solid supports play the key role in the second step. The results show that MNP@PIL/W is highly selective for oxidation of benzyl alcohol and efficiently promotes the Knoevenagel condensation under one-pot condition.

Table 2

The scope of the alcohol substrates was further extended to investigate the general utility of the alcohol oxidation/ Knoevenagel condensation reaction sequence (Table 3). It can be seen that the benzyl alcohols with both electro-donor and electron-withdrawing groups selectively oxidized to the corresponding aldehydes and, in the next step, excellent yield of Knoevenagel product was obtained. However, benzyl alcohols with high steric hindrance need longer reaction times and gave lower yield of products. Secondary and aliphatic alcohols also produce the desired products by this protocol.

Table 3

The recyclability experiment with MNP@PIL/W showed no obvious decrease in catalytic activity after 5 runs (Figure 7 left). However, an increase in reaction time is observed after the 5th run which is attributed to loss of catalyst mass during catalyst separation and recovery. The right

image in Figure 7 shows the leaching test for two steps of the catalytic reaction. In the first experiment, leaching of catalyst was tested in oxidation reaction (line a and b). The results showed that, after catalyst removal, oxidation did not proceed. Line c and d are related to Knoevenagel reactions on benzaldehyde in the presence of MNP@PIL/W and after catalyst removal, respectively. The results clearly show that the catalyst is truly heterogeneous and leaching is negligible under this condition. Moreover, the ICP analysis of the product after hot filtration testing showed no significant amount of tungstate, confirming the results of the leaching experiments.

A possible reaction mechanism for oxidation/Knoevenagel condensation of benzyl alcohol catalyzed by MNP@PIL/W includes 4 steps: (1) oxidation of immobilized WO_4 anions to $\text{WO}_3(\text{O}_2)$, (2) selective oxidation of alcohol to aldehyde, (3) deprotonation of malononitrile by numerous amine groups on the surface of MNP@PIL/W and (4) promotion of the reaction of malononitrile anion and aldehyde by ionic groups on the surface of MNP@PIL/W (Figure S2). The hydrophobic $-\text{CH}_2-$ chains on the surface of the catalyst are important the excellent oxidative activity of the catalyst in water medium as it plays the role of phase transfer catalyst. On the other hand, bis-imidazolium ligand can promote the Knoevenagel condensation with both basic amine function on TCT, which can easily deprotonate malononitrile, and slightly acidic C-H of imidazolium group which can protonate the oxygen of the aldehyde group.

Figure 7

4. Conclusion

In summary, we have shown that MNP@PIL/W is an effective bi-functional catalyst for oxidation/ Knoevenagel condensation of alcohols. The reaction proceeds in the absence of any

phase transfer catalyst in water under mild conditions. Due to the polymeric nature of catalyst, high amounts of tungstate and amine groups were loaded onto the surface of the catalyst which led to a reduction in the amount of catalyst required for the reaction. Considering the versatile structure of MNP@PIL/W catalyst, we believe that more bi-functional catalysts for one-pot tandem reaction can be designed.

Acknowledgements

We are grateful for financial support by the Iran's National Elites Foundation.

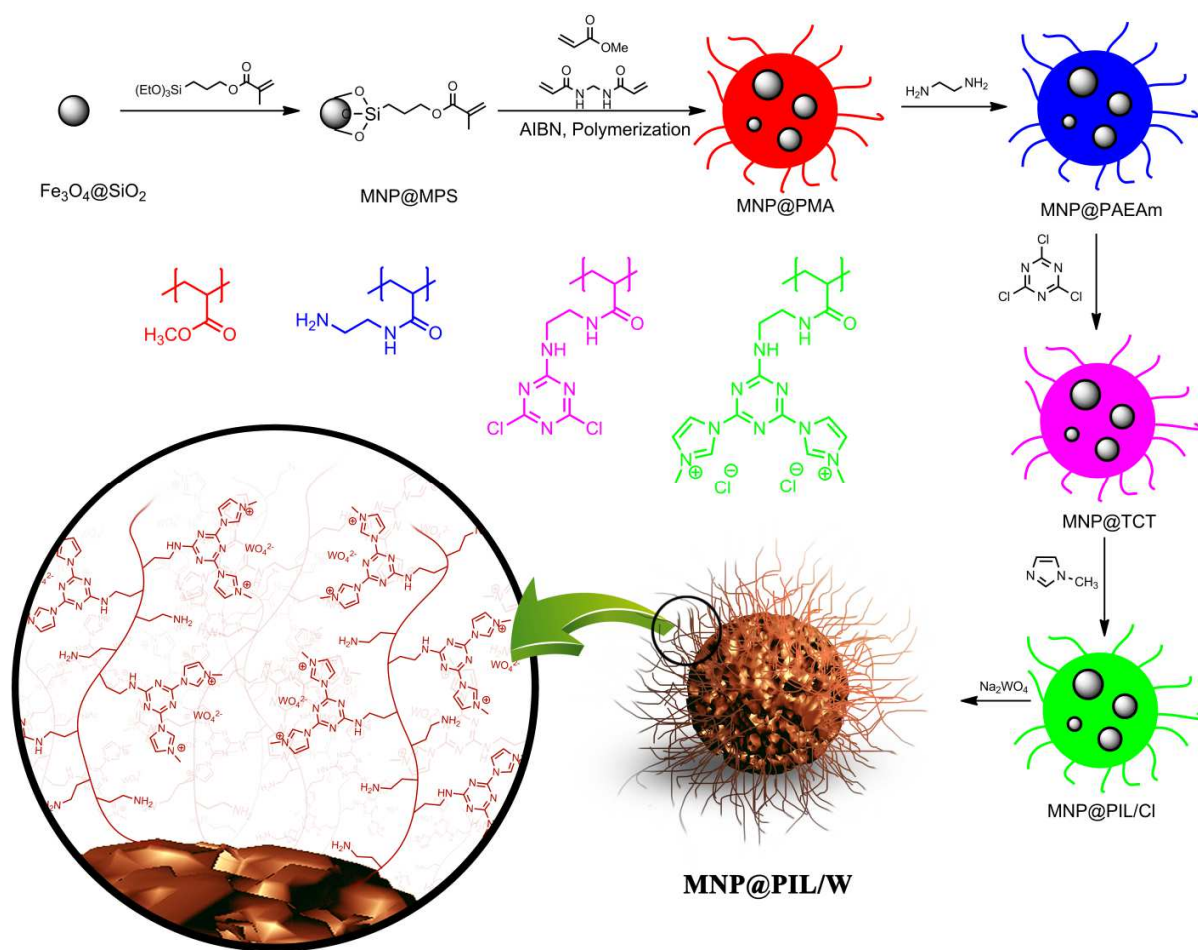
References

1. Plechkova NV and Seddon KR. Chemical Society Reviews 2008;37(1):123-150.
2. Greaves TL and Drummond CJ. Chemical reviews 2015;115(20):11379-11448.
3. Martin RM, Mori DI, Noble RD, and Gin DL. Industrial & Engineering Chemistry Research 2016.
4. Wlazło M, Gawkowska J, and Domańska U. Industrial & Engineering Chemistry Research 2016;55(17):5054-5062.
5. Seifvand N and Kowsari E. Industrial & Engineering Chemistry Research 2016.
6. Salvo AMP, La Parola V, Liotta LF, Giacalone F, and Gruttadauria M. ChemPlusChem 2016;81(5):471-476.
7. Coupillaud P, Vignolle J, Mecerreyes D, and Taton D. Polymer 2014;55(16):3404-3414.
8. Parent JS, Porter AM, Kleczek MR, and Whitney RA. Polymer 2011;52(24):5410-5418.
9. He H, Averick S, Roth E, Luebke D, Nulwala H, and Matyjaszewski K. Polymer 2014;55(16):3330-3338.
10. Welton T. Chemical reviews 1999;99(8):2071-2084.
11. Chen Y, Song H-Y, Lu Y-z, Meng H, Li C, Lei Z-g, and Chen B-h. Industrial & Engineering Chemistry Research 2016.
12. Ogawa T, Yoshida M, Ohara H, Kobayashi A, and Kato M. Chemical Communications 2015;51(69):13377-13380.
13. Kuzmicz D, Coupillaud P, Men Y, Vignolle J, Vendraminetto G, Ambroggi M, Taton D, and Yuan J. Polymer 2014;55(16):3423-3430.
14. Dupont J, de Souza RF, and Suarez PA. Chemical reviews 2002;102(10):3667-3692.

15. Gordon CM. *Applied Catalysis A: General* 2001;222(1):101-117.
16. Amarasekara AS. *Chemical reviews* 2016.
17. Ren J, Wu L, and Li B-G. *Industrial & Engineering Chemistry Research* 2012;51(23):7901-7909.
18. Karimi B and Vafaezadeh M. *Chemical Communications* 2012;48(27):3327-3329.
19. Wu Y, Li Z, and Xia C. *Industrial & Engineering Chemistry Research* 2016;55(7):1859-1865.
20. Zhou H, Yang L, Li W, Wang F, Li W, Zhao J, Liang X, and Liu H. *Industrial & Engineering Chemistry Research* 2012;51(40):13173-13181.
21. Wu B, Hu D, Kuang Y, Liu B, Zhang X, and Chen J. *Angewandte Chemie International Edition* 2009;48(26):4751-4754.
22. Campisciano V, La Parola V, Liotta LF, Giacalone F, and Gruttadauria M. *Chemistry–A European Journal* 2015;21(8):3327-3334.
23. Zhu W, Dai B, Wu P, Chao Y, Xiong J, Xun S, Li H, and Li H. *ACS Sustainable Chemistry & Engineering* 2014;3(1):186-194.
24. Ying A, Liu S, Li Z, Chen G, Yang J, Yan H, and Xu S. *Advanced Synthesis & Catalysis* 2016;358(13):2116-2125.
25. Jiang Y, Guo C, Xia H, Mahmood I, and Liu H. *Industrial & Engineering Chemistry Research* 2008;47(23):9628-9635.
26. Chen S-W, Zhang Z-C, Ma M, Zhong C-M, and Lee S-g. *Organic letters* 2014;16(19):4969-4971.
27. Baig RN and Varma RS. *Chemical Communications* 2013;49(8):752-770.
28. Nazish M, Saravanan S, Khan NuH, Kumari P, Kureshy RI, Abdi SH, and Bajaj HC. *ChemPlusChem* 2014;79(12):1753-1760.
29. Gawande MB, Luque R, and Zboril R. *ChemCatChem* 2014;6(12):3312-3313.
30. Gawande MB, Zboril R, Malgras V, and Yamauchi Y. *Journal of Materials Chemistry A* 2015;3(16):8241-8245.
31. Hemmati K, Sahraei R, and Ghaemy M. *Polymer* 2016;101:257-268.
32. Azgomi N and Mokhtary M. *Journal of Molecular Catalysis A: Chemical* 2015;398:58-64.
33. Candu N, Rizescu C, Podolean I, Tudorache M, Parvulescu V, and Coman S. *Catalysis Science & Technology* 2015;5(2):729-737.
34. Pourjavadi A, Hosseini SH, Moghaddam FM, and Ayati SE. *RSC Advances* 2015;5(38):29609-29617.
35. Moghaddam FM, Ayati SE, Hosseini SH, and Pourjavadi A. *RSC Advances* 2015;5(43):34502-34510.
36. Pourjavadi A, Hosseini SH, Doulabi M, Fakoorpoor SM, and Seidi F. *ACS Catalysis* 2012;2(6):1259-1266.
37. Pourjavadi A, Hosseini SH, and Soleyman R. *Journal of Molecular Catalysis A: Chemical* 2012;365:55-59.
38. Pourjavadi A, Hosseini SH, Moghaddam FM, Foroushani BK, and Bennett C. *Green Chemistry* 2013;15(10):2913-2919.
39. Giacalone F and Gruttadauria M. *ChemCatChem* 2016.
40. Yang J-J, Li C-C, Yang Y-F, Wang C-Y, Lin C-H, and Lee J-T. *RSC Advances* 2016;6(68):63472-63476.
41. Sahle-Demessie E, Gonzalez MA, Enriquez J, and Zhao Q. *Industrial & engineering chemistry research* 2000;39(12):4858-4864.
42. Caron S, Dugger RW, Ruggeri SG, Ragan JA, and Ripin DHB. *Chemical reviews* 2006;106(7):2943-2989.
43. Du YY, Jin Q, Feng JT, Zhang N, He YF, and Li DQ. *Catalysis Science & Technology* 2015;5(6):3216-3225.
44. Azizi N, Khajeh M, and Alipour M. *Industrial & Engineering Chemistry Research* 2014;53(40):15561-15565.
45. Mahamuni NN, Gogate PR, and Pandit AB. *Industrial & engineering chemistry research* 2006;45(26):8829-8836.

46. Hirashita T, Nakanishi M, Uchida T, Yamamoto M, Araki S, Arends IW, and Sheldon RA. *ChemCatChem* 2016;8(16):2704-2709.
47. Hunsen M. *Tetrahedron letters* 2005;46(10):1651-1653.
48. Cherukattu Manayil J, Sankaranarayanan S, Bhadoria DS, and Srinivasan K. *Industrial & Engineering Chemistry Research* 2011;50(23):13380-13386.
49. De Nooy AE, Besemer AC, and van Bekkum H. *Synthesis* 1996;1996(10):1153-1176.
50. Zhu J, Shen Mn, Zhao Xj, Wang Pc, and Lu M. *ChemPlusChem* 2014;79(6):872-878.
51. Salvo AMP, Campisciano V, Beejapur HA, Giacalone F, and Gruttadauria M. *Synlett* 2015;26(09):1179-1184.
52. Beejapur HA, Campisciano V, Giacalone F, and Gruttadauria M. *Advanced Synthesis & Catalysis* 2015;357(1):51-58.
53. Sharma RK, Yadav M, Monga Y, Gaur R, Adholeya A, Zboril R, Varma RS, and Gawande MB. *ACS Sustainable Chemistry & Engineering* 2016;4(3):1123-1130.
54. Noyori R, Aoki M, and Sato K. *Chemical Communications* 2003(16):1977-1986.
55. Strukul G. *Catalytic oxidations with hydrogen peroxide as oxidant: Springer Science & Business Media*, 2013.
56. Zhao P, Zhang M, Wu Y, and Wang J. *Industrial & Engineering Chemistry Research* 2012;51(19):6641-6647.
57. Rahim A, Hasbi M, Forde MM, Jenkins RL, Hammond C, He Q, Dimitratos N, Lopez-Sanchez JA, Carley AF, and Taylor SH. *Angewandte Chemie International Edition* 2013;52(4):1280-1284.
58. Pathan S and Patel A. *Applied Catalysis A: General* 2013;459:59-64.
59. Doherty S, Knight JG, Ellison JR, Weekes D, Harrington RW, Hardacre C, and Manyar H. *Green Chemistry* 2012;14(4):925-929.
60. Shinde VM, Skupien E, and Makkee M. *Catalysis Science & Technology* 2015;5(8):4144-4153.
61. Gogoi SR, Boruah JJ, Sengupta G, Saikia G, Ahmed K, Bania KK, and Islam NS. *Catalysis Science & Technology* 2015;5(1):595-610.
62. Bera PK, Kumari P, Abdi SH, Noor-ul HK, Kureshy RI, Subramanian P, and Bajaj HC. *RSC Advances* 2014;4(106):61550-61556.
63. Bera PK, Gupta N, Abdi SH, Noor-ul HK, Kureshy RI, and Bajaj HC. *RSC Advances* 2015;5(59):47732-47739.
64. Yang J, Shen X, Li Y, Bian L, Dai J, and Yuan D. *ChemCatChem* 2016.
65. Singh S and Patel A. *Industrial & Engineering Chemistry Research* 2014;53(38):14592-14600.
66. Karimi B, Khorasani M, Bakhshandeh Rostami F, Elhamifar D, and Vali H. *ChemPlusChem* 2015;80(6):990-999.
67. Qamar M, Elsayed RB, Alhooshani KR, Ahmed MI, and Bahnemann DW. *ACS applied materials & interfaces* 2015;7(2):1257-1269.
68. Jing L, Shi J, Zhang F, Zhong Y, and Zhu W. *Industrial & Engineering Chemistry Research* 2013;52(30):10095-10104.
69. Kawamura K, Yasuda T, Hatanaka T, Hamahiga K, Matsuda N, Ueshima M, and Nakai K. *Chemical Engineering Journal* 2016;285:49-56.
70. Kundu SK, Mondal J, and Bhaumik A. *Dalton Transactions* 2013;42(29):10515-10524.
71. Sato K, Aoki M, Takagi J, and Noyori R. *Journal of the American Chemical Society* 1997;119(50):12386-12387.
72. Yadav G and Mistry C. *Journal of Molecular Catalysis A: Chemical* 2001;172(1):135-149.
73. Chen C, Yang H, Chen J, Zhang R, Guo L, Gan H, Song B, Zhu W, Hua L, and Hou Z. *Catalysis Communications* 2014;47:49-53.
74. Dhakshinamoorthy A and Garcia H. *ChemSusChem* 2014;7(9):2392-2410.
75. Ang WJ, Chng YS, and Lam Y. *RSC Advances* 2015;5(99):81415-81428.
76. Sarmah B, Srivastava R, Manjunathan P, and Shanbhag GV. *ACS Sustainable Chemistry & Engineering* 2015;3(11):2933-2943.
77. Liu K, Xu Y, Yao Z, Miras HN, and Song YF. *ChemCatChem* 2016;8(5):929-937.

78. Pourjavadi A, Nazari M, and Hosseini SH. RSC Advances 2015;5(41):32263-32271.
79. Zohreh N, Hosseini SH, Pourjavadi A, and Bennett C. RSC Advances 2014;4(91):50047-50055.



Scheme 1. Steps for preparation of MNP@PIL/W.

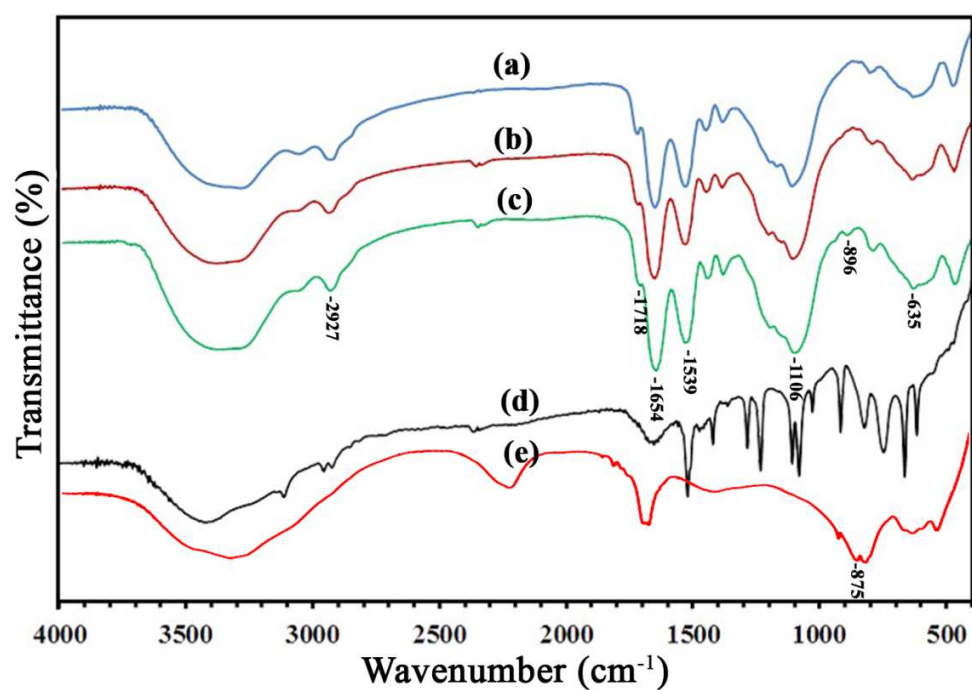


Figure 1. FT-IR spectra of MNP@PAEAm (a), MNP@PTCT (b), MNP@PIL/W (c) *N*-methylimidazole (d) and Na₂WO₄ (e)

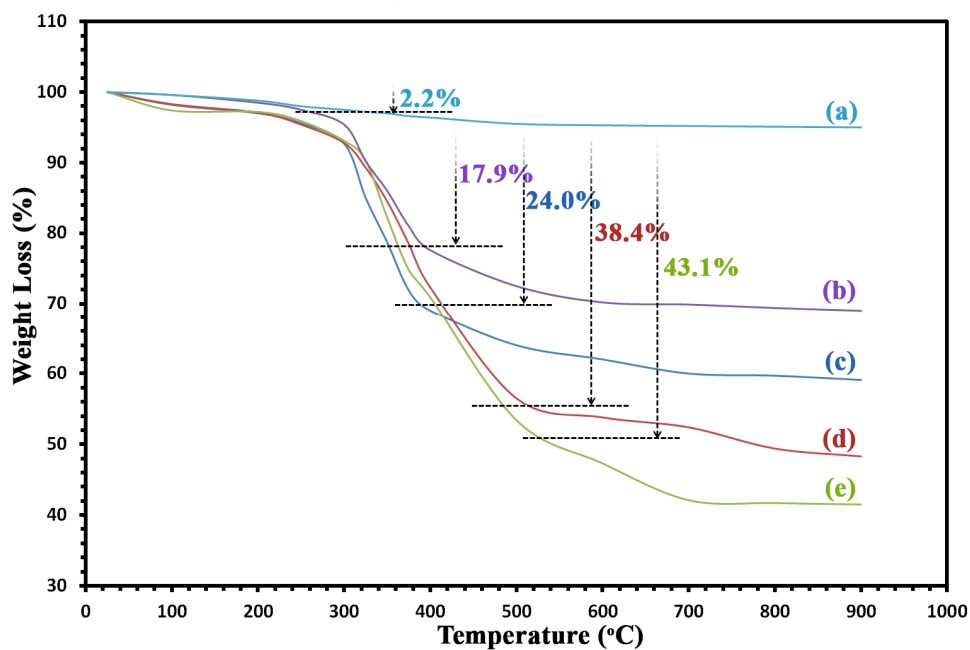


Figure 2. TG analysis of MNP@MPS (a), MNP@PMA (b), MNP@PAEAm (c), MNP@PTCT (d), MNP@PIL/W (e).

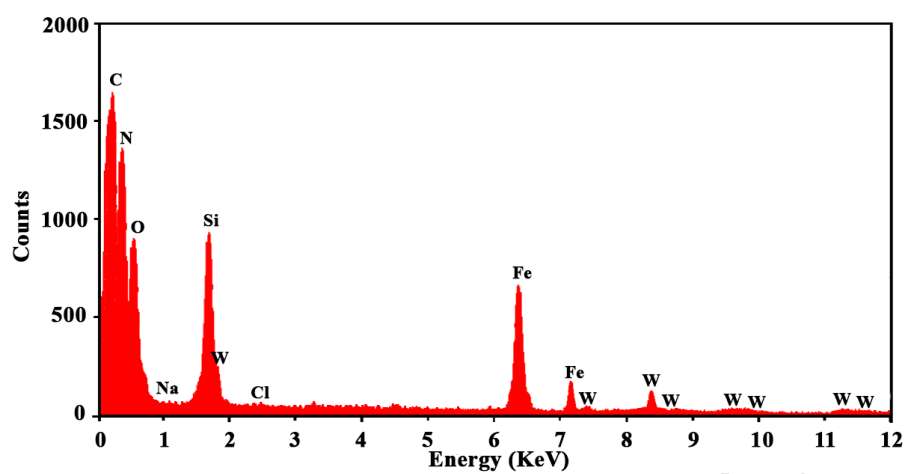


Figure 3. EDS analysis of MNP@PIL/W.

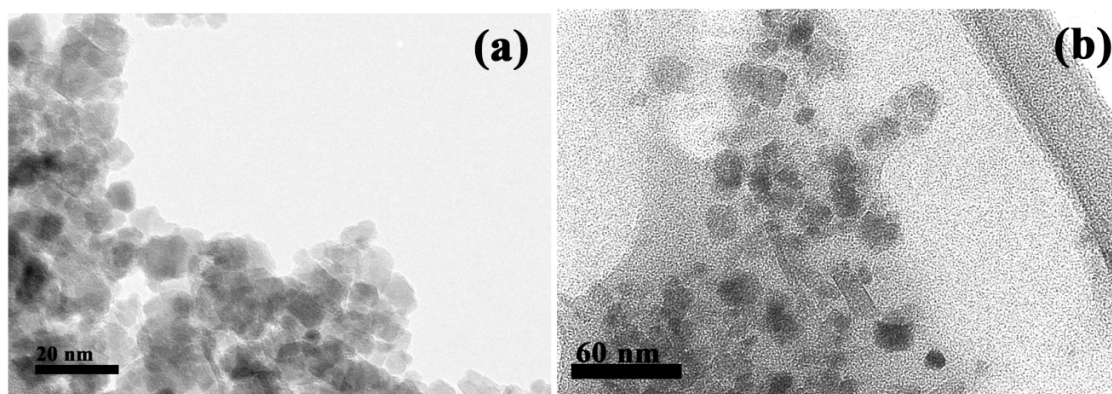


Figure 4. TEM images of Fe₃O₄ nanoparticles (a) and MNP@PIL/W (b).

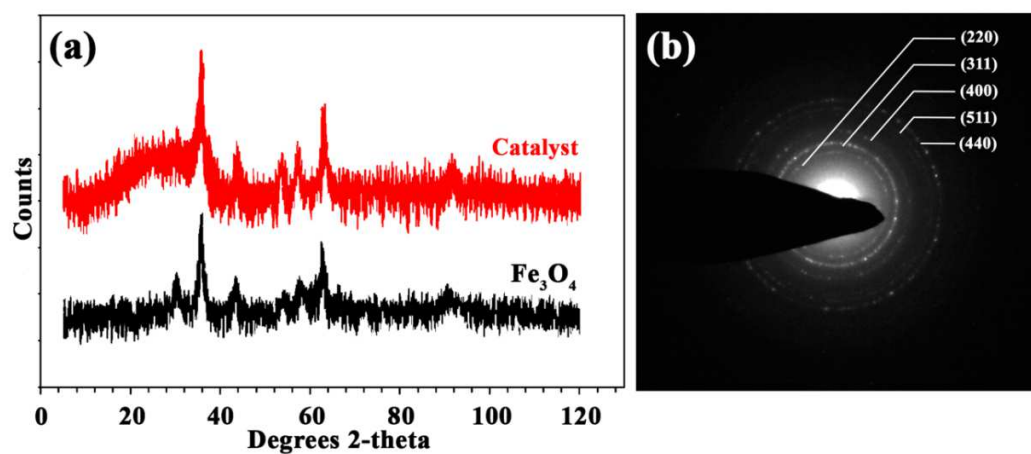


Figure 5. XRD (a) and RDP (b) analysis of MNP@PIL/W.

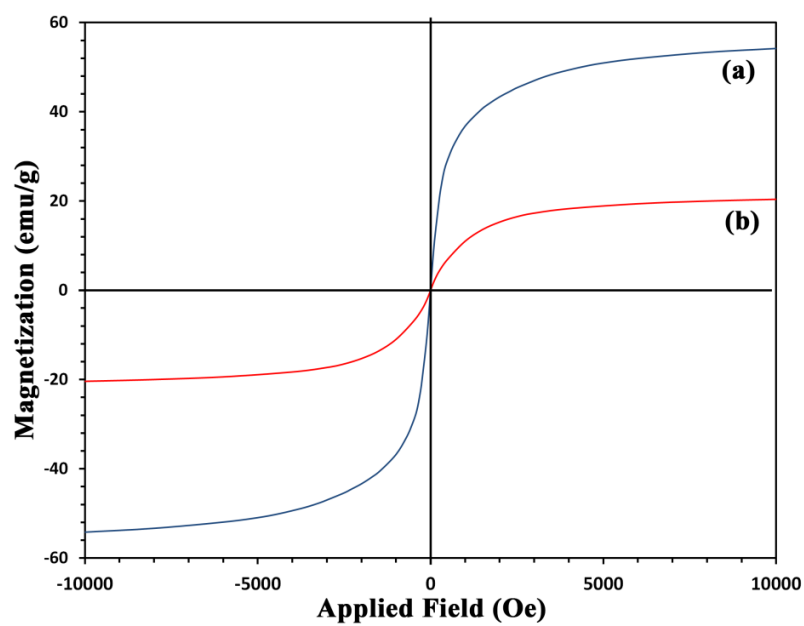


Figure 6. Room temperature magnetization curves of Fe_3O_4 (a) and MNP@PIL/W (b).

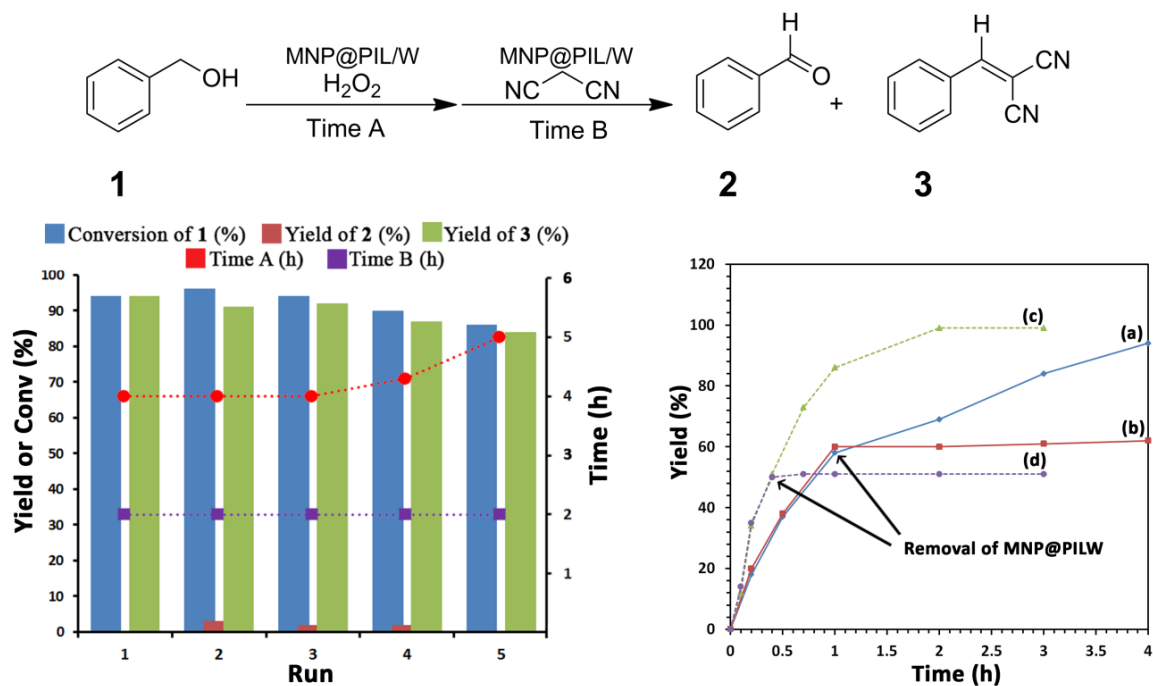


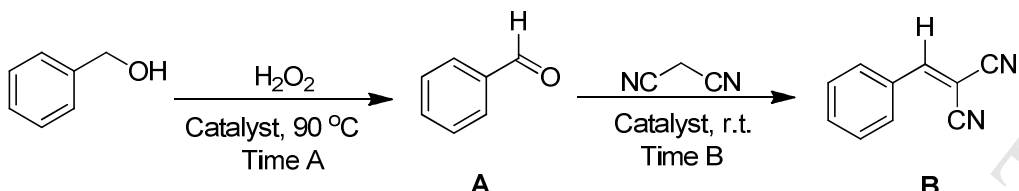
Figure 7. Left: recyclability experiments of MNP@PIL/W (two lines are related to time A and B); Right: leaching test of MNP@PIL/W (a and b: oxidation of **1** to **2** with catalyst and after catalyst removal, respectively; c and d: conversion of **2** to **3** with catalyst and after catalyst removal, respectively).

Table 1. Results of elemental analysis.^a

Sample	C (wt%)	H (wt%)	N (wt%)	Cl (wt%)	W (wt%)	Loading (mmol/g)
MNP@MPS	1.58	1.80	-	-	-	MPS: 0.19
MNP@PMA	11.42	3.71	0.34	-	-	-CO ₂ Me : 1.61 ^b
MNP@PAEAm	13.96	3.88	3.82	-	-	-NH ₂ : 1.24 ^b
MNP@PTCT	14.36	3.32	7.70	6.43	-	TCT: 0.91
MNP@PIL/W	25.30	4.78	9.15	0.59	14.09	WO ₄ : 0.77

^a Weight percent of C, H and N elements were found by CHN analysis and Cl and W were found by XRF.

^b Calculated based on CHN analysis along with TGA data.

Table 2. Control experiment for oxidation/Knoevenagel condensation between benzyl alcohol and malononitrile.^a


Entry	Catalyst	Cat. Loading (mol%)	Solvent	Time (h)		Conv. (%) ^b	Yield (%)	
				A	B		A	B
1	-	-	H ₂ O	12	-	6	2 ^c	-
2	Na ₂ WO ₄	5	H ₂ O	12	3	9	4 ^c	-
3	MNP@PIL/Cl	10 mg	H ₂ O	12	-	13	6 ^c	-
4	MNP@PIL/W	5	H ₂ O	5	2	96	-	96
5	MNP@PIL/W	4	H ₂ O	5	2	94	-	94
6	MNP@PIL/W	3	H ₂ O	5	2	87	-	87
7	MNP@PIL/W	4	H₂O	4	2	94	-	94
8	MNP@PIL/W	4	H ₂ O	4	1	94	12	82
9	MNP@PIL/W	4	H ₂ O	3	2	88	4	84
10	MNP@PIL/W	4	Toluene	6	4	65	49	16
11	MNP@PIL/W	4	CHCl ₃	6	3	79	28	51
12	MNP@PIL/W	4	CH ₃ CN	5	2	84	12	72
13	MNP@PIL/W	4	THF	5	2	76	33	43
14	- ^d	-	H ₂ O	-	5	-	-	-
15	MNP@PIL/Cl ^d	1mg	H ₂ O	-	2	99	-	99
16	PIL/W ^e	4	H ₂ O	4	2	90	-	90

^a Reaction condition: benzyl alcohol (1 mmol), H₂O₂ (1.5 mmol), 90 °C and after A time malononitrile (1.2 mmol) at room temperature for B time. GC yield.

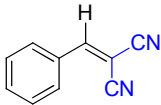
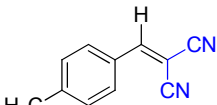
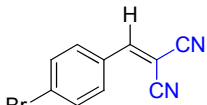
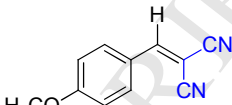
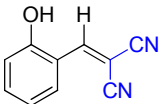
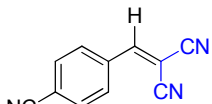
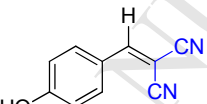
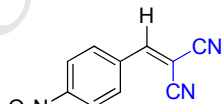
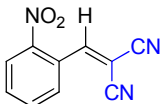
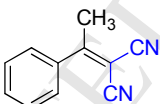
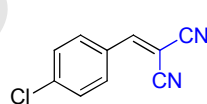
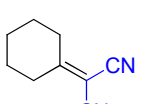
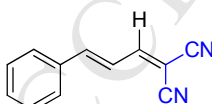
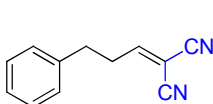
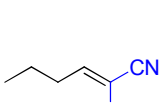
^b Conversions calculated based on initial mmol of benzyl alcohol.

^c Other product is benzoic acid.

^d Reaction started with benzaldehyde (1mmol) and malononitrile (1.2 mmol) at room temperature.

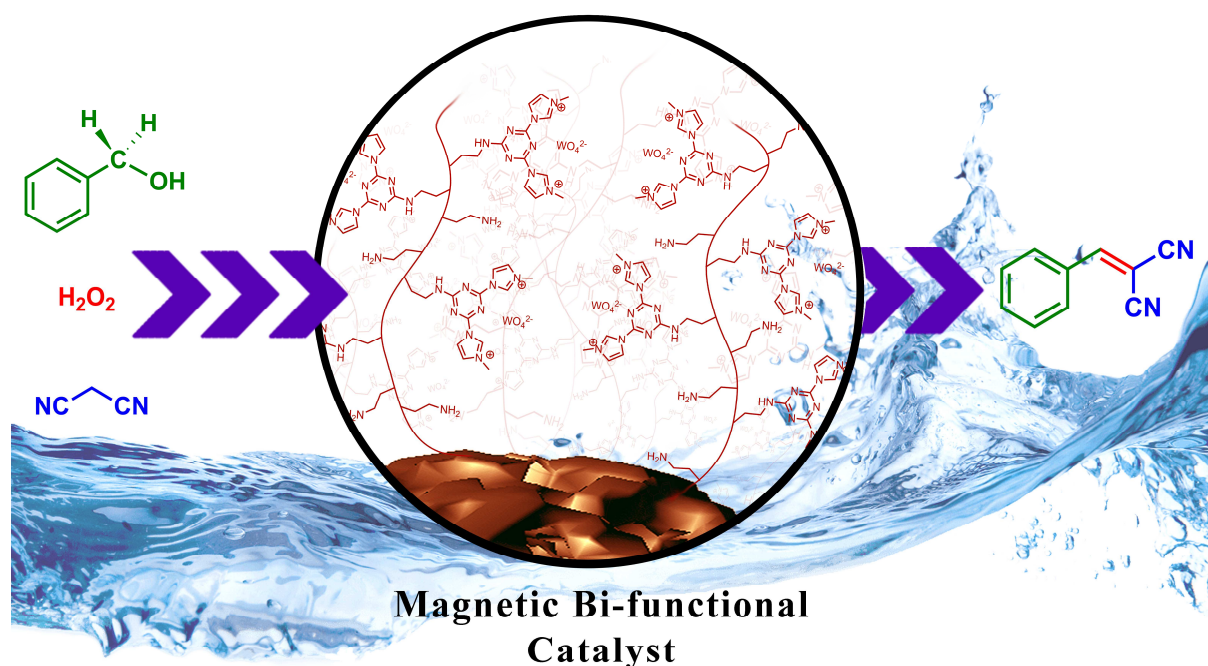
^e Same catalyst without MNPs.

Table 3. Tandem one-pot reaction of oxidation/ Knoevenagel condensation of alcohols catalyzed by MNP@PIL/W.^{a,b}

$\text{R}^1\text{-CH(OH)-R}^2 \xrightarrow[\text{MNP@PIL/W, 90 } ^\circ\text{C, Time A}]{\text{H}_2\text{O}_2} \text{R}^1\text{-C(=O)-R}^2 \xrightarrow[\text{MNP@PIL/W, r.t., Time B}]{\text{NC-CH}_2\text{-CN}} \text{R}^1\text{-C(=CH-CN)-C(=O)-R}^2$	
 <p>Time A: 4h Time B: 2h Conv. : 94% Yield : 94%(87%)</p>	 <p>Time A: 4h Time B: 2h Conv. : 96% Yield : 94%</p>
 <p>Time A: 5h Time B: 2h Conv. : 93% Yield : 92%</p>	 <p>Time A: 6h Time B: 2.5h Conv. : 90% Yield : 86%</p>
 <p>Time A: 8h Time B: 3h Conv. : 79% Yield : 65%</p>	 <p>Time A: 5h Time B: 3h Conv. : 91% Yield : 90%</p>
 <p>Time A: 3.5h Time B: 1h Conv. : 98% Yield : 98%(93%)</p>	 <p>Time A: 5h Time B: 1.5h Conv. : 95% Yield : 95%(91%)</p>
 <p>Time A: 9h Time B: 5h Conv. : 39% Yield : 25%(23%)</p>	 <p>Time A: 5h Time B: 3h Conv. : 91% Yield : 90%</p>
 <p>Time A: 3h Time B: 3h Conv. : 88% Yield : 81%(75%)</p>	 <p>Time A: 10h Time B: 5h Conv. : 83% Yield : 80%</p>
 <p>Time A: 6h Time B: 1h Conv. : 99% Yield : 95%</p>	 <p>Time A: 9h Time B: 5h Conv. : 78% Yield : 69%</p>
	 <p>Time A: 12h Time B: 6h Conv. : 90% Yield : 84%</p>

^a Reaction condition: Alcohol (0.5 mmol), MNP@PIL/W (4 mol%), H₂O₂ (0.75 mmol), H₂O (2 mL) at 90 °C and after A hours malononitrile (0.6 mmol) at room temperature for B hours.

^b GC yield. The values in the parenthesis refer to the isolated yield.



- 1- Easy synthesis of WO_4^{2-} decorated bi-functional heterogeneous catalyst
- 2- Selective oxidation of alcohols to aldehyde followed by Knoevenagel condensation with malononitrile using 4 mol% tungstate catalyst/ H_2O_2 in water
- 3- High catalytic activity and excellent selectivity of the catalyst in water medium
- 4- Easy separation (external magnet) and high reusability of the catalyst